Available online at www.sciencedirect.com

ScienceDirect

Procedia Engineering 130 (2015) 552 – 559

Procedia Engineering

www.elsevier.com/locate/procedia

14th International Conference on Pressure Vessel Technology

Finite Element Modelling of Welding Residual Stress and Its Influence on Creep Behavior of a 2.25Cr-1Mo-0.25V Steel Cylinder

Y. Zhou[a,*], X.D. Chen[a], Z.C. Fan[a], S.X. Rao[b]

[a]*National Engineering Technical Research Center on PVP Safety, Hefei General Machinery Research Institute, Hefei, Anhui, 230031, China*
[b]*School of Mechanical Engineering, Anhui University of Technology, Ma'anshan, Anhui, 243032, China*

Abstract

Thermo-mechanical finite element analysis was performed to predict the residual stress distribution in a single-U butt weld of a 2.25Cr-1Mo-0.25V steel cylinder using ANSYS. An axisymmetric model of the cylinder with a wall thickness of 150 mm, having a 55-pass weld, was adopted in the study to reduce computation complexity. The influence of welding residual stress on creep behavior of the welded joint subjected to internal pressure under operation condition was investigated using the continuum damage mechanics (CDM) theory. The results showed that the distribution of welding residual stress in the multi-pass weld was quite complex, and the residual stress can be relaxed to a lower level in a short time during creep, which can accelerate the creep damage of the welded joint.

Peer-review under responsibility of the organizing committee of ICPVT-14

Keywords: finite element analysis; welding residual stress; continuum damage mechanics; creep

1. Introduction

Low alloy ferritic Cr-Mo steels are widely used to manufacture hydroprocessing reactors in petrochemical industry[1-4]. As compared to the conventional 2.25Cr-1Mo steel, the vanadium-modified steel 2.25Cr-1Mo-0.25V exhibits better material performance, including the mechanical properties at room temperature and at elevated temperatures, the resistance to high-temperature hydrogen attack and hydrogen embrittlement, etc. Hence, it is

* Corresponding author. Tel.: +8613855528827; fax: +8605552316515.
E-mail address: yuzhou@buaa.edu.cn

Peer-review under responsibility of the organizing committee of ICPVT-14
doi:10.1016/j.proeng.2015.12.264

preferentially selected in the design of large-scale and heavy-wall hydroprocessing reactors, in order to achieve the goal of light-weight design.

It is well known that welding residual stress plays an important role in structural integrity, influencing the mechanical behavior of components. For example, reheat cracking relate to welding residual stress were reported to occur in hydroprocessing reactors[5,6]. Due to the complexity of welding process which is involving mass transportation, thermal conduction, metallurgy and mechanics, many studies on numerical simulation of welding by finite element method (FEM) have been conducted in the last few decades, in order to accurately predict the deformation and residual stress induced by welding[7-11]. However, little research work on the influence of welding residual stress on creep damage of vanadium-modified Cr-Mo steel components has been carried out.

In the present study, the welding residual stress in a single-U butt weld of a 2.25Cr-1Mo-0.25V steel cylinder was predicted by thermo-mechanical finite element analysis. The influence of welding residual stress on the creep damage of the welded joint was investigated using the continuum damage mechanics (CDM) theory, where a physically-based creep damage constitutive model was adopted to describe the material damage evolution during creep.

2. Finite element modelling of welding residual stress

Simulation of welding residual stress was performed on a single-U multi-pass butt weld of a 2.25Cr-1Mo-0.25V steel cylinder. The detailed geometry of the welded joint is shown in Fig. 1. The welded joint with 55 passes is welded using submerged arc welding (SAW). The preheating temperature is 200°C and the inter-pass temperature is controlled in the range of 160-250°C. The welding voltage and current are 30V and 500A, respectively. The thermal physical parameters of 2.25Cr-1Mo-0.25V steel is assumed to be the same as those of 2.25Cr-1Mo, due to lack of experimental data at high temperatures. Fig. 2 combines a set of these physical parameters and thermal mechanical properties plotted against temperature[12].

It has been reported that 2D model can accurately predict the thermal cycles and residual stress, and an axisymmetric model is considered to be sufficient to represent a cylinder weld[10,12]. Hence, the axisymmetric FE model of the heavy-wall cylinder, containing 3126 nodes and 3072 elements, is used in an effort to reduce the computation time for the 55-pass weld. Fig. 3 shows the mesh within and around the fusion zone. A fine mesh is used in the fusion zone and the mesh away from the weld line center gradually becomes coarser.

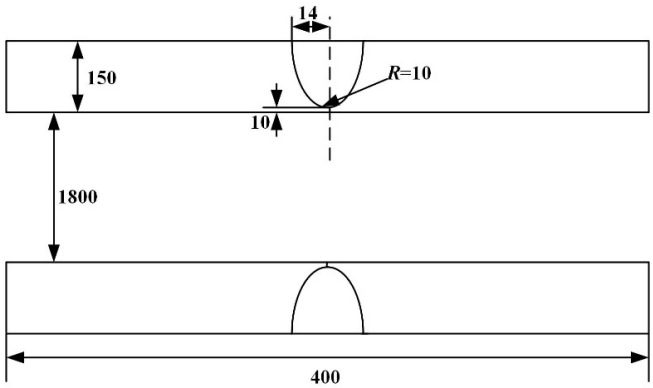

Fig. 1. Geometry of the 2.25Cr-1Mo-0.25V steel cylinder with a single-U butt weld (unit: mm).

The welding residual stress was simulated by a sequentially coupled thermo-mechanical finite element program using ANSYS. Firstly, the calculation of temperature field was performed by the nonlinear transient heat conduction analysis, and the supply of weld material was simulated by the so-called “element birth/death technique”. A volumetric heat source model is employed, and the total net heat input Q can be obtained as:

$$Q = \eta UI / v \tag{1}$$

where η represents the efficiency factor, v is the welding speed, U and I are arc voltage and current, respectively. The efficiency factor for SAW welding process is assumed to be 0.95. Meanwhile, heat loss due to heat transfer that dominates at high temperatures and thermal radiation that dominates at low temperatures is considered. A combined heat transfer coefficient h which is temperature dependent is utilized to account for these two kinds of heat loss, and can be obtained as follows[13]:

$$h = \begin{cases} 0.0668T \times 10^{-6}\ \mathrm{W/mm^2} & 0 < T < 500^{\circ}\mathrm{C} \\ (0.231T - 82.1) \times 10^{-6}\ \mathrm{W/mm^2} & T > 500^{\circ}\mathrm{C} \end{cases} \tag{2}$$

where T is temperature. It is worthy of note that the heat transfer boundaries were time-varied, due to the addition of new elements which simulates the material filling during welding. In addition, the latent heat of fusion is considered to model the thermal effects induced by solidification.

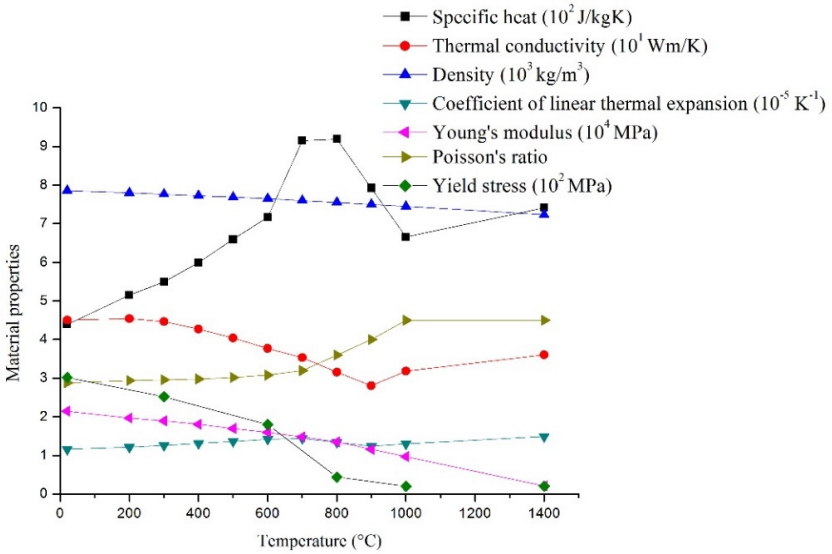

Fig. 2. Mechanical and thermal physical properties plotted against temperature.

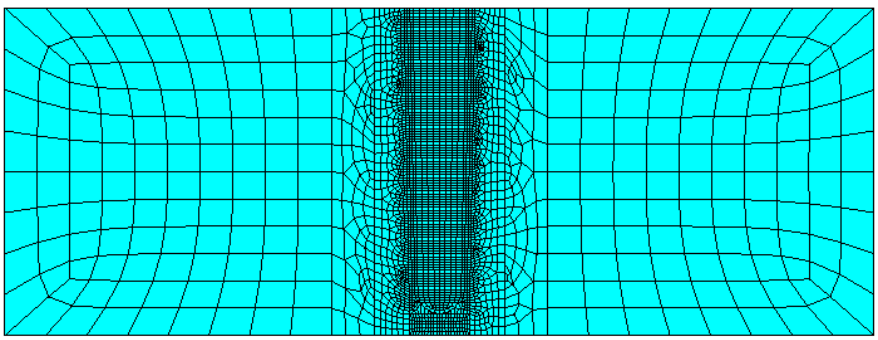

Fig. 3. FE model of the welded joint.

Then, the temperature distribution obtained from the thermal analysis was applied as thermal body load in the subsequent structural analysis to calculate the welding residual stress field. Temperature-dependent material properties are shown in Fig. 2 and the bilinear isotropic hardening model is assumed. In addition, the displacements in the y-direction of the nodes at the ends of the cylinder are constrained.

Fig. 4(a) shows the contour of the complex hoop residual stress of the multi-pass welded joint. It can be seen that the hoop residual stress on the inner surface is compressive while it changes to tensile on the outer surface. It is due to the shrinkage of the material in and near the fusion zone, resulting in the formation of bending moment during cooling. The maximum residual stress occurs in the fusion zone near the outer surface. Fig. 4(b) shows the contour of axial residual stress. It is tensile in nature, and the location of the maximum stress is close to that of the maximum hoop stress. Fig. 5-Fig.6 show the distribution of hoop stress and axial stress in the longitudinal direction on the inner surface and outer surface, respectively. It can be seen that the axial residual stress is generally larger than the hoop stress on the inner surface. The axial and hoop residual stress on the outer surface are basically tensile stress. The maximum stress occurs in the fusion zone or the HAZ region. The stress is gradually decreased with the increase of the distance away from the weld center line.

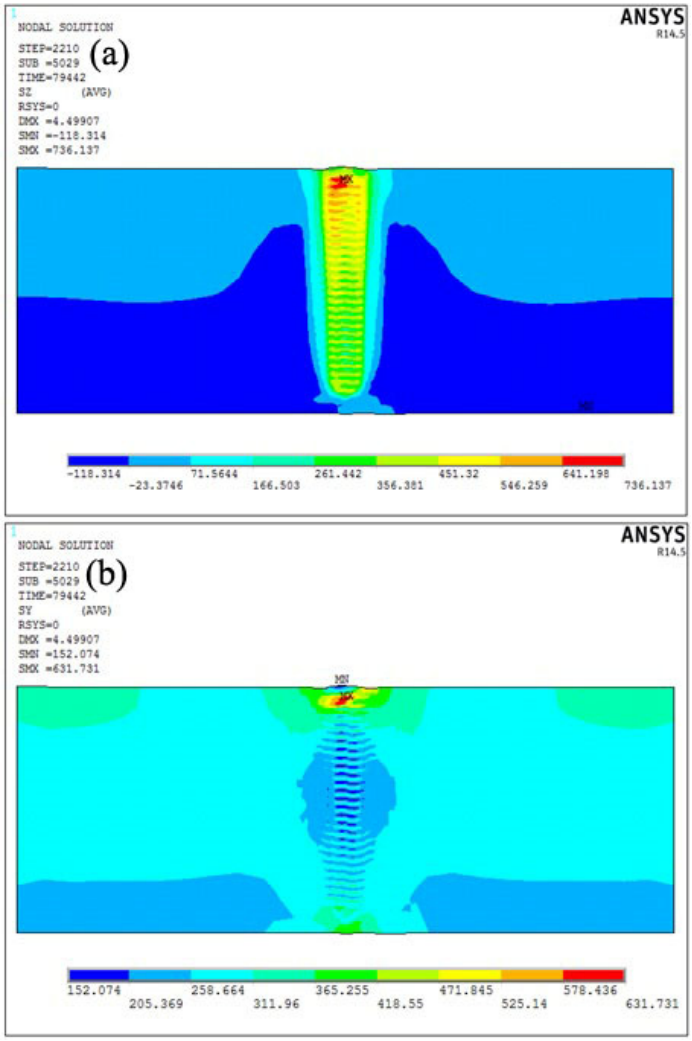

Fig. 4. Contour of (a) hoop and (b) axial residual stress of the welded joint (unit: MPa).

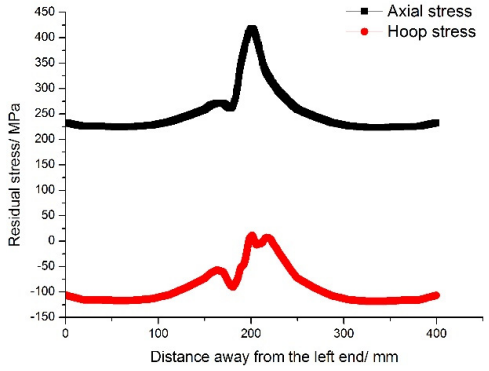

Fig. 5. Residual stress distribution on the inner surface.

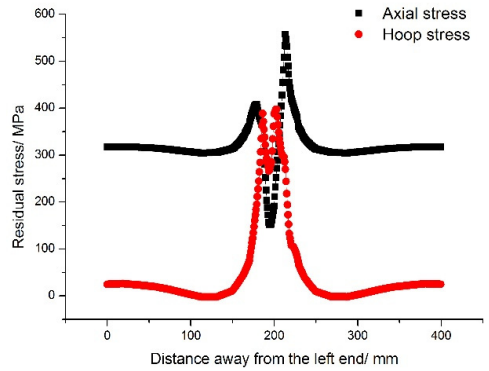

Fig. 6. Residual stress distribution on the outer surface.

3. Influence of welding residual stress on creep damage

It has been proved that continuum damage mechanics (CDM) together with FEM can be used to predict the creep behavior of complex structures[2,3]. In our previous work, creep damage evolution of hydroproceesing reactors and stress relaxation behavior were analyzed using CDM and FEM[14]. Therefore, the influence of welding residual stress on creep damage of the welded joint was also studied by this combined method. The creep damage constitutive model for low alloy ferritic steels, involving two types of material damage (i.e., carbide coarsening and grain boundary cavitation), is given as follows[15]:

$$\begin{cases} \dot{\varepsilon}_c = A\sinh\left[\dfrac{B\sigma(1-H)}{(1-\phi)(1-\omega)}\right] \\ \dot{H} = \dfrac{h\dot{\varepsilon}}{\sigma}\left(1-\dfrac{H}{H^*}\right) \\ \dot{\phi} = \dfrac{K_c}{3}(1-\phi)^4 \\ \dot{\omega} = C\dot{\varepsilon} \end{cases} \tag{3}$$

where $\dot{\varepsilon}_c$ is the creep strain rate, σ is the applied stress, H represents the strain hardening behavior during primary creep, ϕ and ω are two damage variables which represent carbide coarsening and grain boundary cavitation, respectively. A, B, C, h, H^*, K_c are material constants which can be determined by the experimental creep data. Table 1 lists the six material constants of 2.25Cr-1Mo-0.25V steel at the operation temperature of 454°C[14]. The CDM model was then implemented into a user-defined subroutine for creep, using Fortran language and the user programmable features (UPFs) of ANSYS.

Table 1. Material constants of 2.25Cr-1Mo-0.25V steel at 454°C.

A / h^{-1}	B / MPa^{-1}	C / -	h / MPa	H^* / -	K_c / h^{-1}
8.2896×10^{-10}	0.1213	4.8929	1.5546×10^{5}	0.7469	4.1640×10^{-7}

The welding residual stress as an initial stress for creep analysis was imported into the FE model, using the "INISTATE" command in ANSYS. Creep simulation of the welded joint was performed through the user-defined subroutine under the internal pressure of 21.7MPa at 454°C. Fig. 7 shows the hoop stress distribution of the welded joint subjected to internal pressure for 10h, taking the welding residual stress into consideration. It can be clearly seen that the welding residual stress is relaxed drastically in the initial stage of creep, and the hoop stress distribution in the welded joint is influenced by the distribution of welding residual stress, as compared with Fig. 4.

Fig. 8(a)-(b) show the creep damage distribution of the joint serviced for 262800h, which is the design life (i.e. 30 years), with and without the consideration of welding residual stress. It is indicated that creep damage in the welded joint is strongly related to welding residual stress. The maximum creep damage occurs in the heat affected zone (HAZ) on the outer surface, where the maximum welding residual stress is present, resulting in the occurrence of type IV cracking. The maximum creep damage considering welding residual stress is 13% larger than that without consideration of the residual stress. Therefore, it can be inferred that the welding residual stress can accelerate the creep damage and its influence on the integrity of the welded joint could not be neglected.

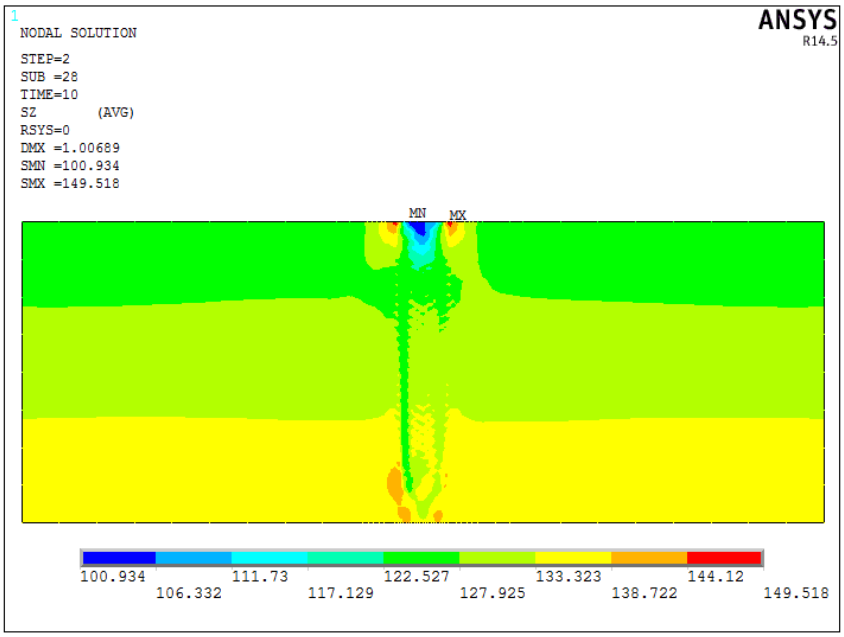

Fig. 7. Contour of hoop stress of the welded joint serviced for 10h (unit: MPa).

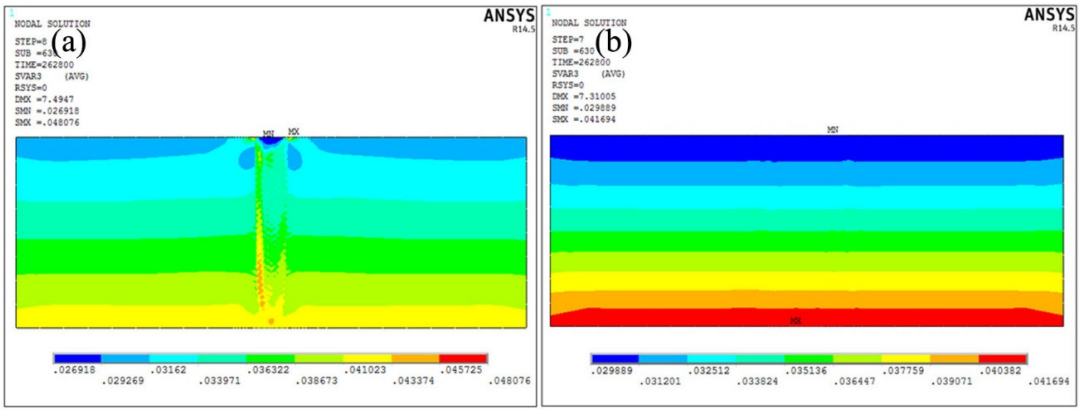

Fig. 8. Contour of the creep damage variable ω after service of 30 years (a) with and (b) without the consideration of welding residual stress.

4. Conclusions

Welding residual stress and its influence on the creep damage of the 2.25Cr-1Mo-0.25V steel heavy-wall cylinder with a 55-pass weld was studied using CDM and FEM in the present paper. The hoop residual stress on the inner surface is compressive while it changes to tensile on the outer surface. The axial residual stress is tensile, and the location of the maximum stress is close to that of the maximum hoop stress.

The welding residual stress of the welded joint is relaxed greatly during primary creep, and creep damage is strongly related to welding residual stress. The maximum creep damage considering welding residual stress, occurring in the HAZ on the outer surface, is 13% larger than that without consideration of the residual stress. It can be concluded that the welding residual stress plays a very important role in the creep response of the welded joint, resulting in the acceleration of creep damage.

Acknowledgements

Financial support from the National Basic Research Program of China (973 Program, No. 2015CB057603) and the National Nature Science Foundation of China (No. 51301001) is gratefully acknowledged.

References

[1] X.D. Chen, J. Cui, Z.C. Fan, X.H. Zhang, W.H. Guan, B.N. Shou, T.J. Xie, Design, manufacture and maintenance of high-parameter pressure vessels in China, Proceedings of the ASME 2014 Pressure Vessels & Piping Conference, ASME, California, 2014, PVP2014-28569.

[2] D.R. Hayhurst, I.W. Goodall, R.J. Hayhurst, D.W. Dean, Lifetime predictions for high-temperature low-alloy ferritic steel weldments, The Journal of Strain Analysis for Engineering Design, 40 (2005) 675-701.

[3] R.J. Hayhurst, D.W. Dean, CDM prediction of creep failure modes in thin and thick section Cr-Mo-V butt-welded pipes under combined internal pressure and end loads at temperatures in the range 540–620°C, Fatigue & Fracture of Engineering Materials & Structures, 34 (2011) 689–707.

[4] N.S. Cheruvu, Degradation of mechanical properties of Cr-Mo-V and 2.25Cr-1Mo steel components after long-term service at elevated temperatures, Metallurgical Transactions A, 20 (1989) 87-97.

[5] Y.C. Han, X.D. Chen, Z.C. Fan, H.Q. Bu, Y. Zhou, Reheat cracking sensitivity of CGHAZ in vanadium-modified 2.25Cr1Mo welds, Proceedings of the ASME 2014 Pressure Vessels & Piping Conference, ASME, California, 2014, PVP2014-28706.

[6] J.E. Indacochea, G.S. Kim, Reheat cracking studies on simulated heat-affected zones of CrMoV turbine rotor steels, Journal of Materials Engineering and Performance, 5 (1996) 353-364.

[7] D. Deng, FEM prediction of welding residual stress and distortion in carbon steel considering phase transformation effects, Materials & Design, 30 (2009) 359–366.

[8] D. Deng, H. Murakawa, Finite element analysis of temperature field, microstructure and residual stress in multi-pass butt-welded 2.25Cr–1Mo steel pipes, Computational Materials Science, 43 (2008) 681-695.
[9] D. Deng, H. Murakawa, Numerical simulation of temperature field and residual stress in multi-pass welds in stainless steel pipe and comparison with experimental measurements, Computational Materials Science, 37 (2006) 269-277.
[10] A. Yaghi, T.H. Hyde, A.A. Becker, W. Sun, J.A. Williams, Residual stress simulation in thin and thick-walled stainless steel pipe welds including pipe diameter effects, International Journal of Pressure Vessels and Piping, 83 (2006) 864-874.
[11] J.R. Cho, B.Y. Lee, Y.H. Moon, C.J. Van Tyne, Investigation of residual stress and post weld heat treatment of multi-pass welds by finite element method and experiments, Journal of Materials Processing Technology, 155-156 (2004) 1690–1695.
[12] D. Deng, S. Kiyoshima, H. Serizawa, H. Murakawa, Numerical investigation on welding residual stress in 2.25Cr-1Mo steel pipes, Transactions of JWRI, 36 (2007) 73-90.
[13] B. Brickstad, B.L. Josefson, A parametric study of residual stresses in multi-pass butt-welded stainless steel pipes, International Journal of Pressure Vessels and Piping, 75 (1998) 11–25.
[14] Y. Zhou, X.D. Chen, Z.C. Fan, J. Dong, Creep simulation of the hydroprocessing reactor using a physically-based CDM model, Proceedings of the ASME 2015 Pressure Vessels & Piping Conference, ASME, Boston, 2015, PVP2015-45416.
[15] R. Mustata, D.R. Hayhurst, Creep constitutive equations for a 0.5Cr 0.5 Mo 0.25V ferritic steel in the temperature range 565 °C–675 °C", International Journal of Pressure Vessels and Piping, 82 (2005) 363–372.